

Density of states, compositional short-range order, and stability of amorphous Zr_xCu_{1-x} alloys

H. -J. Eifert and B. Elschner

*Institut für Festkörperphysik, Technische Hochschule, D-6100 Darmstadt,
Federal Republic of Germany*

K. H. J. Buschow

Philips Research Laboratories, 5600 MD Eindhoven, The Netherlands

(Received 16 November 1981)

We report on ^{63}Cu , ^{65}Cu , and ^{91}Zr NMR measurements of the metallic glass Zr_xCu_{1-x} ($0.38 \leq x \leq 0.72$), studied together with magnetic measurements. We discuss our results in terms of a two-band model with local densities of states and show that the d -electron density of states increases with increasing x . The averaged quadrupole coupling constant was determined at the ^{65}Cu and the ^{91}Zr sites. From the concentration dependence of the ^{91}Zr quadrupole coupling constant it was derived that near 70 at. % Zr appreciable compositional short-range order exists.

I. INTRODUCTION

Much attention has been focused recently on the studies of the electronic structure of metallic glasses. In this context the system Zr-Cu, which is a classical one with a rather wide concentration range, was the object of several photoemission experiments^{1,2} and computer calculations using the self-consistent augmented-spherical-wave method.³ It was shown, among other things, that the Zr d band lies close to the Fermi level and that the Cu d -band peaks are shifted to higher binding energies. In the present investigation we have studied for the first time the ^{63}Cu , ^{65}Cu , and ^{91}Zr NMR in the amorphous alloys Zr_xCu_{1-x} ($0.38 \leq x \leq 0.72$). From the NMR Knight-shift results and from the results of magnetic measurements important conclusions can be drawn regarding the density of states near the Fermi energy. We will investigate whether or not the change in the density of states with increasing x has any relationship to the stability of the amorphous alloys.

The possibility of observing nuclear quadrupole interactions by means of NMR opens the possibility of obtaining information about the angular distribution of the local atomic arrangement in these alloys. This information usually cannot be obtained from x-ray and neutron diffraction or from extended x-ray absorption fine-structure measurements. We will use our NMR results to answer the question concerning how accurately the atomic

arrangements in amorphous alloys can be described by means of a dense random packing of hard spheres (DRPHS) or whether a description favoring compositional short-range ordering between the atoms is more appropriate.

II. EXPERIMENTAL DETAILS

The amorphous Zr_xCu_{1-x} alloys investigated in this study ($x=0.38, 0.44, 0.50, \text{ and } 0.72$) were prepared by melt spinning on a copper wheel in an atmosphere of purified argon. The melt spinning was performed with alloy buttons of the desired composition that had been prepared before by arc melting. Small parts of the amorphous ribbons (about 2-mm broad and 30- μm thick) were investigated by x-ray diffraction. All alloys were found to have x-ray diagrams characteristic of the amorphous state. Sharp diffraction lines indicating the presence of some crystalline material were absent. The thermal behavior of the alloys was studied on a differential scanning calorimeter (DSC). The heating rates were varied from 0.5 to 100 K/min.

For the NMR investigations the amorphous ribbons were cut into pieces of about 0.5 mm, reduced to a semifluid consistency with silicon oil to increase the effective sample volume. The NMR equipment used was a Bruker BKR 322 S spin-echo spectrometer, operated in combination with an Oxford Instruments superconducting magnet.

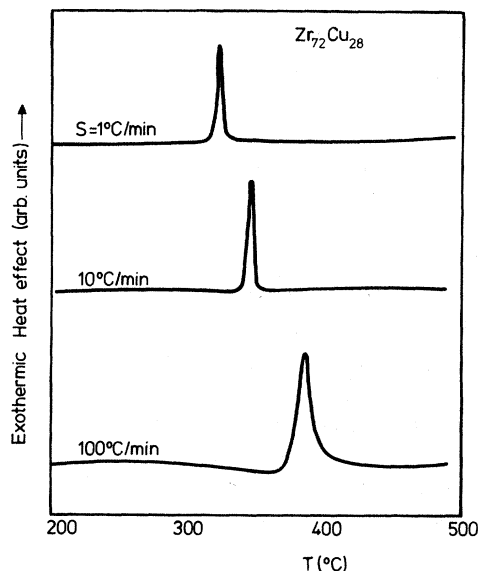


FIG. 1. DSC traces of the amorphous alloy $Zr_{72}Cu_{28}$ obtained at three different heating rates.

The ^{63}Cu and the ^{65}Cu resonances were measured by choosing a normal phase-sensitive detection and a boxcar integrator in order to improve the signal-to-noise ratio. For the detection of the weak ^{91}Zr resonance it was necessary to make use of a technique by means of which the value of the echo heights could be obtained independent of the phase of the signal. We therefore used a two-channel main amplifier (Bruker Quadro receiver) with two signals phase-sensitively detected relative to refer-

ences having a constant phase relation of 90° . These signals were fed by two fast analog-to-digital converters (ADC's, Bruker Transistore) into a computer (Nicolet BNC 12) in order to calculate $(S_\rho^2 + S_{\rho+90^\circ})^{1/2}$. The field sweep velocity in the case of the ^{91}Zr resonance was about $3 \cdot 10^{-4}$ T/min. All NMR measurements were performed at 4 K. The time lapse between sample preparation and NMR measurements was of the order of a few days. The susceptibility of the samples was measured with a Foner-type magnetometer in the temperature range between 2.9 and 270 K at a field of 10 kG.

III. EXPERIMENTAL RESULTS AND INTERPRETATION

A. Thermal stability

Typical results of DSC measurements are shown in Fig. 1. X-ray analysis of samples that had been heated to temperatures above the strong exothermic heat effect showed that crystallization had taken place. The crystallization temperature T_x defined as the temperature corresponding to the peak of the strong exothermic heat effect is seen to vary considerably with the heating rate s applied. The dependence of T_x on s can be used to derive values of the activation energy ΔE determining the crystallization rates. Two methods were used. Follow-

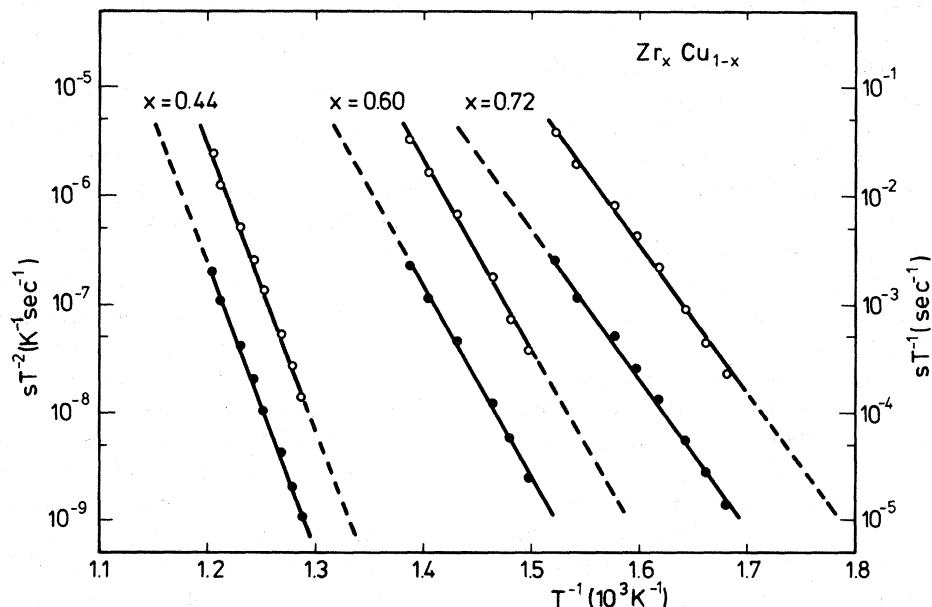


FIG. 2. Dependence of the crystallization temperature observed in various amorphous Zr_xCu_{1-x} alloys on the heating rate s . The open circles and the left-hand scale refer to the method of Kissinger. The solid circles and the right-hand scale refer to the method of Boswell. (See text.)

TABLE I. Comparison of the activation energies for crystallization derived by means of the method of Kissinger (ΔE) and the method of Boswell ($\Delta E'$).

Zr _x Cu _{1-x}	ΔE (eV)	$\Delta E'$ (eV)
$x = 0.72$	2.73	2.70
0.60	3.60	3.58
0.50	4.11	4.21
0.44	5.40	5.19
0.38	5.37	5.26

ing Kissinger's method we plotted $\ln(s/T_x^2)$ vs $1/T_x$. As seen in Fig. 2 these plots are straight lines, showing that the crystallization process can be described by a single activation law. The activation energies ΔE derived from the slopes of these plots are listed in Table I. According to Boswell it is more appropriate to plot $\ln(s/T_x)$ vs $1/T_x$. Such plots are included in Fig. 2. Also in this case the activation energies ΔE are derived from the slope of the straight lines. In order to be able to compare both methods we have increased the lengths of the straight lines in Fig. 2 somewhat by means of a broken part. It can be seen from Fig. 2 that there is hardly any difference in slope. The ΔE values derived by the two different methods show a difference of only a few percent.

B. Quadrupole interaction

In the nonmagnetic amorphous alloy the various NMR probes (^{63}Cu , ^{65}Cu , ^{91}Zr) experience different

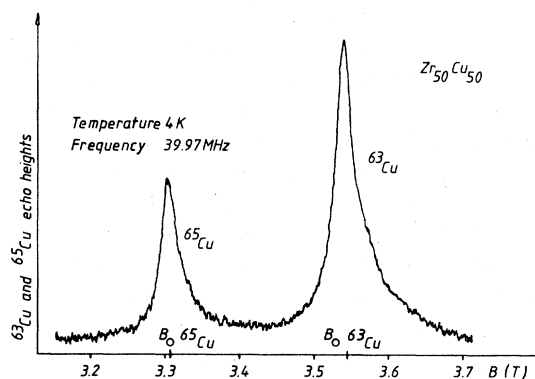


FIG. 3. Spin-echo spectrum of ^{63}Cu and ^{65}Cu obtained at 4 K in the amorphous alloy $\text{Zr}_{50}\text{Cu}_{50}$.

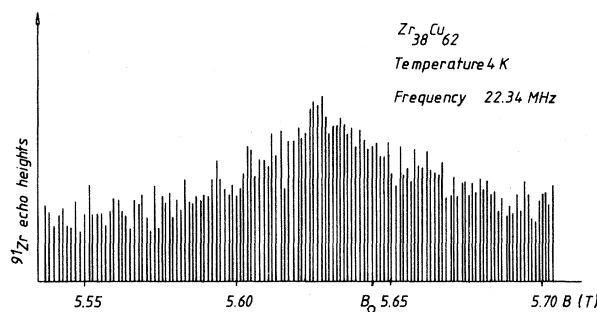


FIG. 4. Spin-echo spectrum of ^{91}Zr obtained at 4 K in amorphous $\text{Zr}_{38}\text{Cu}_{62}$.

electric field gradients owing to a distribution of different local environments. This is why the line shape of the spectra is a superposition of many quadrupolar split powder patterns with different splittings. In first-order perturbation calculation the $+\frac{1}{2} \leftrightarrow -\frac{1}{2}$ transition does not give rise to a quadrupole shift, and the resulting powder pattern is symmetrical relative to the resonance field H_{res} . The second-order perturbation calculation shifts the $+\frac{1}{2} \leftrightarrow -\frac{1}{2}$ transition so the powder spectrum is no longer symmetrical. Figure 3 shows the ^{65}Cu and the ^{63}Cu resonance of amorphous $\text{Zr}_{50}\text{Cu}_{50}$ and Fig. 4 the ^{91}Zr resonance of amorphous $\text{Zr}_{38}\text{Cu}_{62}$. Because all of these resonances are not symmetrical and have their center of gravity shifted to higher fields, we conclude that we see mainly a broad distribution of superimposed powder patterns of the $+\frac{1}{2} \leftrightarrow -\frac{1}{2}$ transition. The field of the center of gravity $H_{\text{c.g.}}$ relative to the resonance field H_{res} can be expressed as follows⁶:

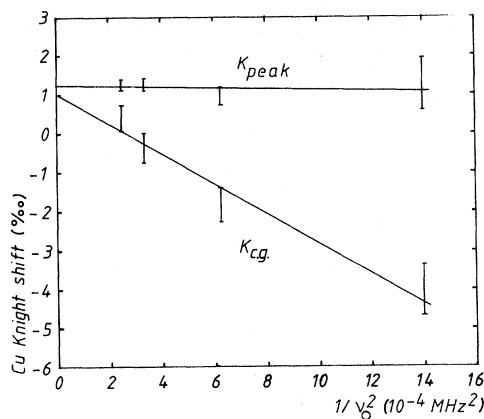


FIG. 5. Frequency dependence of the ^{63}Cu Knight shift at 4 K in amorphous $\text{Zr}_{50}\text{Cu}_{50}$. For the meaning of K_{peak} and $K_{\text{c.g.}}$ see text.

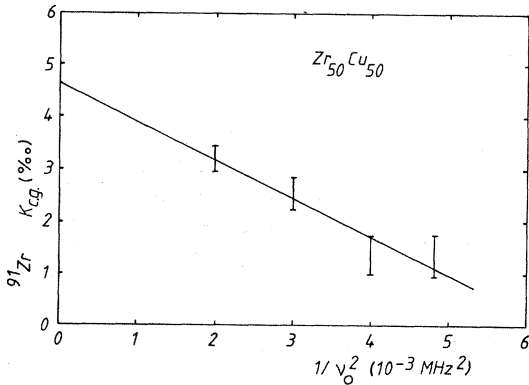


FIG 6. Frequency dependence of the ^{91}Zr Knight shift at 4 K in amorphous $\text{Zr}_{50}\text{Cu}_{50}$. For the meaning of $K_{\text{c.g.}}$ see text.

$$H_{\text{c.g.}} - H_{\text{res}} = \left[\frac{3}{40} \frac{2I+3}{4I^2(2I-1)} \left(\frac{e^2qQ}{\gamma h} \right)^2 \right] \times \left[1 + \frac{\eta^2}{3} \right] \frac{1}{H_{\text{res}}} \quad (1a)$$

or

$$H_{\text{c.g.}} - H_{\text{res}} = C/H_{\text{res}}, \quad (1b)$$

where C represents the expression in square brackets in Eq. (1a). The constants appearing in this expression represent the following: I is the nuclear spin, γ the gyromagnetic ratio of the nuclei, e^2qQ/h the quadrupole coupling constant in frequency units, and η the asymmetry parameter.

If H_{dm} represents the (Cu or Zr) resonance field in diamagnetic reference the Knight shift K is defined by

$$H_{\text{res}} \cong H_{\text{dm}}(1-K). \quad (2)$$

It follows from Eq. (1a) that there is a shift of $H_{\text{c.g.}}$ relative to H_{res} to higher fields which is proportional to $1/H_{\text{res}}$. Accordingly, the Knight shift

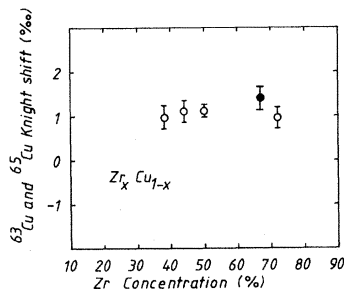


FIG 7. Concentration dependence of the ^{63}Cu (^{65}Cu) Knight shift (K_0 ; see text) in amorphous $\text{Zr}_x\text{Cu}_{1-x}$ alloys (open circles) and crystalline Zr_2Cu (solid circle).

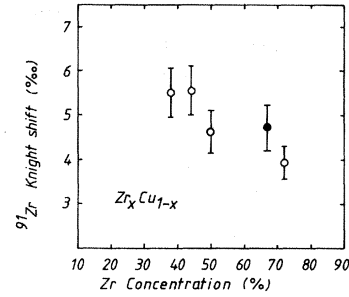


FIG 8. Concentration dependence of the ^{91}Zr Knight shift (K_0 , see text) in amorphous $\text{Zr}_x\text{Cu}_{1-x}$ (open circles) crystalline Zr_2Cu (solid circle).

corresponding to the center of gravity of the distribution of resonances in the amorphous alloy ($\bar{K}_{\text{c.g.}}$) is proportional to $1/H_{\text{dm}}^2$:

$$\bar{K}_{\text{c.g.}} = \frac{H_{\text{dm}} - H_{\text{c.g.}}}{H_{\text{dm}}} = \frac{H_{\text{dm}} - H_{\text{res}}}{H_{\text{dm}}} - \frac{H_{\text{c.g.}} - H_{\text{res}}}{H_{\text{dm}}}, \quad (3a)$$

$$K_{\text{c.g.}} \approx K_0 - \frac{\bar{C}}{H_{\text{dm}}^2} = K_0 - \frac{\bar{C}\gamma}{\nu_0^2}, \quad (3b)$$

where ν_0 is the measuring frequency.

A study of the frequency dependence of $K_{\text{c.g.}}$ should therefore lead to the parameters desired, i.e., to the Knight shift and the average quadrupole coupling constant. Note that the former quantity, but not the latter, can also be derived from the frequency dependence of the maximum of the echo height K_{peak} . Examples of experimental results for the various amorphous alloys are shown in Figs. 5 and 6. These results are in accordance with the behavior expected on the basis of Eq. (3b). As the asymmetry parameter η fulfills the condition $0 \leq \eta \leq 1$, the influence of the $1 + \eta^2/3$ term appearing in \bar{C} [Eqs. (1a) and (1b)] is rather insignificant and merely increases the experimental error of the averaged quadrupole coupling constant. From the value of \bar{C} derived by means of the behavior of the ^{65}Cu resonance in amorphous $\text{Zr}_{50}\text{Cu}_{50}$ (Fig. 5) we obtained $e^2qQ/h = 11.5 \pm 2.3$ MHz or $\nu_Q = 5.7 \pm 1.2$ MHz, where $\nu_Q = 3e^2qQ/2I(2I-1)h$. The ^{63}Cu resonance is less suited to evaluation owing to the presence of small Al and Na resonances originating from the sample holder or the glue.

Using the $Q(^{65}\text{Cu}) = -0.195 \times 10^{-24}$ cm² of the copper nuclear quadrupole moment⁷ we are able to calculate the average electric field gradient as $\langle \delta^2V/\delta z^2 \rangle_{\text{Zr}} = (2.4 \pm 0.5) \times 10^{17}$ V/cm². This re-

TABLE II. Quadrupole constants, quadrupole frequencies, and electric field gradients from ^{91}Zr NMR in various amorphous $\text{Zr}_x\text{Cu}_{1-x}$ alloys and in crystalline Zr_2Cu . The value $Q(^{91}\text{Zr}) = -0.21 \times 10^{-24} \text{ cm}^2$ was taken from Büttgenbach *et al.* [Z. Phys. A 286, 125 (1978)].

	$\text{Zr}_{38}\text{Cu}_{62}$	$\text{Zr}_{44}\text{Cu}_{56}$	$\text{Zr}_{50}\text{Cu}_{50}$	$\text{Zr}_{72}\text{Cu}_{28}$	Zr_2Cu
$\frac{e^2qQ}{h}/\text{MHz}$	11.9 ± 2.4	11.9 ± 2.4	10.3 ± 2.1	7.2 ± 1.4	6.4 ± 0.9
ν_Q/MHz	1.8 ± 0.4	1.8 ± 0.4	1.6 ± 0.3	1.1 ± 0.2	1.0 ± 0.1
$\frac{\partial^2 V}{\partial z^2} (10^{17} \text{V/cm}^2)$	2.3 ± 0.5	2.3 ± 0.5	2.0 ± 0.4	1.4 ± 0.3	1.3 ± 0.2

sult can be compared, for instance, with the Cu resonance in a single crystal of Cu alloyed with 1 at. % Pd leading to $\nu_Q = 3.1 \text{ Mhz}$.⁸ The fact that ν_Q in the amorphous $\text{Zr}_{50}\text{Cu}_{50}$ alloy is considerably larger than in the Cu: Pd single crystal is not surprising in view of the lack of atomic order and the higher concentration of the second component in the former. Of even more influence is perhaps the large difference in electronic properties between Cu and Zr whereas Cu and Pd are much more similar.

The results derived from the behavior of the ^{91}Zr resonance are collected in Table II. These results can be compared with those of Hoiki *et al.*⁹ who observed the ^{91}Zr resonance in hexagonal closed-packed (hcp) Zr metal. These authors determined a quadrupole coupling constant of $e^2qQ/h = 18.7 \text{ MHz}$. The Zr coupling constant in glassy $\text{Zr}_x\text{Cu}_{1-x}$ is seen to be substantially smaller than in Zr metal. This is true for the quadrupole coupling constant of $\text{Zr}_{72}\text{Cu}_{28}$, in particular, which is the lowest one compared to the other amorphous alloys. Note that the value obtained for $\text{Zr}_{72}\text{Cu}_{28}$ does not differ much from that obtained in crystalline Zr_2Cu .

C. Knight shift and magnetic susceptibility

According to Eq. (3b) the values of the Knight shift K in the various amorphous alloys can be de-

rived from the frequency dependence of the center of gravity of the Cu and Zr resonances by plotting $K_{c.g.}$ vs ν_0^{-2} and extrapolating to $\nu_0^{-2} \rightarrow 0$. The intercepts on the vertical axes of graphs such as those shown for $\text{Zr}_{50}\text{Cu}_{50}$ in Figs. 5 and 6 are listed in Table III and have been plotted as a function of concentration in Figs. 7 and 8. It is seen that the Cu Knight shift remains roughly constant with increasing Zr concentration, whereas the Zr Knight shift gives rise to a strong decrease.

The magnetic susceptibility measured on the amorphous alloys was corrected for diamagnetic contributions^{10,11} by using a weighted average of the diamagnetic susceptibilities of the pure elements. Values of $\chi - \chi_{dm}$ obtained in this way are included in Table III. It can be derived from these results that the Pauli paramagnetism increases with Zr concentration.

Below we will analyze the Knight-shift and susceptibility data by means of a two-band model composed of a narrow d band and a broad s,p band. The assumption of a two-band model of the type mentioned is reasonable in view of the electronic structure of the composing elements and in view of current band-structure calculations on related metal systems.^{12,13} Amamou *et al.*¹ and also Oelhafen *et al.*² found that the hybridization between the Cu $3d$ states and the Zr $4d$ states leads to a narrowing of the Cu d -electron density of states in the alloy together with a shift to lower energies. The d -electron density of states near the Fermi en-

TABLE III. Zr and Cu Knight shift (in $^\circ |_{\infty}$) and total magnetic susceptibility corrected for diamagnetism (in 10^{-5} emu/mol) in several amorphous $\text{Zr}_x\text{Cu}_{1-x}$ alloys and crystalline Zr_2Cu .

	$\text{Zr}_{38}\text{Cu}_{62}$	$\text{Zr}_{44}\text{Cu}_{56}$	$\text{Zr}_{50}\text{Cu}_{50}$	$\text{Zr}_{72}\text{Cu}_{28}$	Zr_2Cu
K_0^{Zr}	5.50 ± 0.55	5.54 ± 0.55	4.63 ± 0.46	3.91 ± 0.39	4.73 ± 0.52
K_0^{Cu}	0.98 ± 0.25	1.10 ± 0.25	1.11 ± 0.17	0.96 ± 0.25	1.40 ± 0.26
$\chi_{\text{exp}} - \chi_{\text{dm}}$	6.90 ± 0.35	8.18 ± 0.41	8.43 ± 0.42	13.08 ± 0.66	

ergy E_F is composed predominantly of the Zr d electrons. For this reason we assume in our analysis that the d -electron contributions to K and χ are due only to the Zr d electrons. An argument in favor of this assumption is the concentration dependence of χ shown in Table III.

We can represent the measured susceptibility χ by means of the following expression:

$$\chi - \chi_{\text{dm}} = \frac{2}{3}\chi_{s,p} + x(\chi_d + \chi_{vv}). \quad (4)$$

The d -electron susceptibility χ_d and the molar orbital susceptibility χ_{vv} are due to the Zr atoms only.

The Knight shifts at the site of the Cu atoms and the Zr atoms K_0^{Cu} and K_0^{Zr} are given by

$$K_0^{\text{Cu}} = K_{s,p}^{\text{Cu}} = \epsilon_{\text{Cu}} a_{s,p}^{\text{Cu}} \chi_{s,p}, \quad (5)$$

$$K_0^{\text{Zr}} = K_{s,p}^{\text{Zr}} + K_d^{\text{Zr}} + K_{vv}^{\text{Zr}}, \quad (6a)$$

$$K_0^{\text{Zr}} = \epsilon_{\text{Zr}} a_{s,p}^{\text{Zr}} \chi_{s,p} + a_d \chi_d + a_{vv} \chi_{vv}. \quad (6b)$$

The quantities ϵ_{Cu} and ϵ_{Zr} are weighting factors distributing the s,p band susceptibility between the atomic volumes of the NMR probe atoms:

$$\epsilon_{\text{Cu}} = \frac{V_{\text{Cu}}}{xV_{\text{Zr}} + (1-x)V_{\text{Cu}}}, \quad (7)$$

$$\epsilon_{\text{Zr}} = \frac{V_{\text{Zr}}}{xV_{\text{Zr}} + (1-x)V_{\text{Cu}}}.$$

The atomic volumes V_{Cu} and V_{Zr} were assumed to be spherical and to have radii equal to $r_{\text{Cu}} = 1.27 \text{ \AA}$ and $r_{\text{Zr}} = 1.60 \text{ \AA}$.¹⁴ The factor $a_{s,p}$ represents the effective s -electron hyperfine coupling parameter. Following the results of similar analyses and assuming an s,p band where the s and p electrons contribute equal parts to $\chi_{s,p}$, one finds $a_{s,p} = 0.45a_s$ (Refs. 6 and 15) where a_s is the s -electron hyperfine coupling constant in the absence of p electrons.

The d -electron hyperfine field coupling constant a_d was obtained from the relationship $a_d \approx -0.1a_s$.¹⁶ The coupling constant for a_{vv} in Zr was calculated from the mean value of a_{vv} in ⁹⁵Mo and ¹⁰⁹Rh reported in Refs. 17 and 18, each value being first adapted to the appropriate value of $\langle r^{-3} \rangle$.¹⁹ The various hyperfine field coupling parameters used by us are listed in Table IV.

The values of $\chi_{s,p}$, χ_d and χ_{vv} obtained for the different concentrations by solving Eqs. (4)–(6) are given in Table V. Inspection of the results given in Table V shows that the d -electron density of states is a factor 6–8 greater than the s,p electron density. This result is rather similar to that ob-

TABLE IV. Hyperfine field coupling constants used in the present investigation.

	a_s $\left[\frac{\text{mol}}{\text{emu}} \right]$	a_d $\left[\frac{\text{mol}}{\text{emu}} \right]$	a_{vv} $\left[\frac{\text{mol}}{\text{emu}} \right]$
Cu	484		
Zr	358	36	40

tained for Zr metal by Hioki *et al.*,⁹ who found a d -electron density of states 9 times larger than the s,p density of states. It can also be seen from the table that χ_{vv} is larger than χ_d by a factor of 3. This result also resembles that found by Hioki *et al.* in Zr metal.⁹

We can summarize the results of our analysis by stating that in the amorphous Zr-Cu alloys a narrow d band is present, having a large density of states near E_F . The d -electron density is due to the d electrons contributed by the Zr atoms. This leads to Pauli paramagnetism that increases with increasing Zr concentration and, owing to the negative sign of the d -electron hyperfine field coupling constant, to a decreasing ⁹¹Zr Knight shift with increasing Zr concentration. Qualitatively, our results are in agreement with results derived from specific-heat measurements, showing density of states increasing with Zr concentration.²⁰

IV. CONCLUDING REMARKS

It is frequently assumed that amorphous alloys are relatively stable when the electronic structure of the amorphous alloys meets certain requirements. In several papers Nagel and Tauc^{21–23} have pointed out that a close analogy exists between the stability of so-called Hume-Rothery electron compounds and the stability of amorphous alloys of a certain valence electron concentration. In Hume-Rothery compounds the crystal structure gives rise to Brillouin-zone planes, and the interaction of these planes with the electron states near the Fermi surface can lead to a lowering of the density of states and hence to an increased stability. In amorphous alloys the situation is more complex. Nagel and Tauc argue that here a similar interaction can occur between the electron states near E_F and the first pronounced maximum in the structure factor $S(q)$ associated with the Fourier transform of the atomic radial distribution function. To be more specific, stable amorphous alloys are expected when the Fermi wave vector k_F approaches the wave vector $\frac{1}{2}q_m$ where q_m corresponds to the maximum in the wave-vector-

TABLE V. Comparison of the relative magnitude of the various contributions of the magnetic susceptibility in various amorphous Zr_xCu_{1-x} alloys (in emu/mole).

	$Zr_{38}Cu_{62}$	$Zr_{44}Cu_{56}$	$Zr_{50}Cu_{50}$	$Zr_{72}Cu_{28}$
$\chi_{s,p} 10^{-6}$	6.25	7.32	7.61	7.60
$\chi_d 10^{-5}$	3.68	4.08	4.37	5.93
$\chi_w 10^{-4}$	1.34	1.34	1.14	1.16
χ_w/χ_d	3.6	3.3	2.6	2
$\chi_d/\chi_{s,p}$	5.9	5.6	5.7	7.8

dependent structure factor $S(q)$. In terms of the free-electron approach (where k_F^3 is proportional to the number of valence electrons) this has a consequence that the energetically favorable situation $2k_F \approx q_m$ can always be reached at a given concentration of an amorphous alloy in which a monovalent metal is combined with a polyvalent metal. Near this particular concentration one expects simultaneously the presence of a reduced density of states near E_F and an enhanced resistance against crystallization (higher crystallization temperatures). The decrease of the crystallization temperature with increasing x in Zr_xCu_{1-x} ($0.32 \leq x \leq 0.5$) has been taken to reflect the increase in k_F with x , E_F moving away from the favorable region of a low density of states.²⁴ The results of the present investigation strongly oppose this view since our susceptibility and Knight-shift data show convincingly that increasing x (corresponding to decreasing crystallization temperature^{25,26}) is accompanied by a pronounced increase in the density of states rather than by a decrease. Here we wish to emphasize again the fact that amorphous alloys are metastable in character and that their resistance against crystallization is a matter of reaction kinetics and activation energies rather than a matter of relative stabilities as assumed in the Nagel and Tauc model. Even if the reduction in $N(E_F)$ of alloys satisfying the condition $2k_F \approx q_m$ would lead to an increase in stability amounting to a substantial portion of the difference in stability between the amorphous and crystalline state [typical values are $\Delta H_{\text{cryst}} = 1.2$ kcal/g at. (Refs. 25 and 27)], the activation energies derived in Sec. III ($\Delta E \approx 100$ kcal/g at.) are about 2 orders of magnitude larger than this stability increase. Hence, from this point of view, it is rather unlikely that the Nagel and Tauc criterion can give a correct description of the stability of amorphous alloys. Comparable results, refuting the applicability of the Nagel and Tauc criterion, were also obtained in amorphous alloys based on metalloids.²⁸

Finally, we wish to emphasize the fact that we found an averaged quadrupole coupling constant in Zr_xCu_{1-x} that decreases with increasing x and that is substantially smaller in all cases than the value observed in crystalline Zr metal. The quadrupole constant is a measure of the local electric field gradient and as such can give information about the local environment of a given atom. It has been widely accepted for many years that the atomic arrangement in an amorphous alloy can be described by means of DRPHS. In such alloys one expects considerable deviations from cubic symmetry and consequently large values of the quadrupole constant. This is true, in particular, if the valences of the surrounding metal atoms are much different. Our results are therefore rather surprising, since they indicate that near the concentration $x = 0.7$, in particular, the local atomic arrangements responsible for the field gradient are quite symmetrical. The local structural arrangement may be related to that of the cubic bcc phase observed in the crystallization of $Zr_{75}Cu_{25}$,²⁶ or to that in crystalline Zr_2Cu . Here we recall that in addition to the NMR resonances in amorphous material we investigated the crystalline compound Zr_2Cu also (Figs. 7 and 8, Tables II and III). We showed that the Knight shifts are almost the same as we would expect by interpolation of the amorphous data, indicating that the density of states is not much different in the crystalline and amorphous states. Even more important is the fact that we observed a clear splitting of the $+\frac{1}{2} \leftrightarrow -\frac{1}{2}$ transitions due to a well-defined electrical field gradient at the Cu or at Zr sites, the value of the field gradient in the crystalline structure and the averaged value in amorphous $Zr_{72}Cu_{28}$ being very similar. The tendency of the quadrupole constants of the amorphous alloys to decrease with x and approach the value observed in crystalline Zr_2Cu can be taken as strong evidence for the occurrence of compositional short-range ordering in these alloys, refuting the random packing assumed in the

DRPHS model. Our results are in concord with those of a similar investigation reported by Panissod *et al.*²⁹

ACKNOWLEDGMENTS

The authors are indebted to Professor Dr. E. Dormann for many stimulating discussions and to

O. Krahl for the susceptibility measurements. They wish to thank Professor Dr. G. V. Minningerode and Dr. K. Samwer for sending us their specific-heat data prior to publication. The NMR equipment used in Darmstadt was provided by the Bundesministerium für Bildung und Wissenschaft and by the Deutsche Forschungsgemeinschaft (SFB 65—Festkörperspektroskopie—Darmstadt, Frankfurt).

-
- ¹A. Amamou and G. Krill, *Solid State Commun.* **28**, 957 (1978).
- ²P. Oelhafen, E. Hauser, H.-J. Güntherodt, and K. H. Bennemann, *Phys. Rev. Lett.* **43**, 1134 (1979).
- ³J. Kübler, K. H. Bennemann, R. Lapka, F. Rösel, P. Oelhafen, and H.-J. Güntherodt, *Phys. Rev. B.* **23**, 5176 (1981).
- ⁴H. E. Kissinger, *Anal. Chem.* **29**, 1702 (1957).
- ⁵F. G. Boswell, *J. Therm. Anal.* **18**, 353 (1980).
- ⁶G. C. Carter, L. H. Bennett, and D. J. Kahan, *Prog. Mat. Sci.* **20**, 1 (1977).
- ⁷G. H. Fuller and V. W. Cohen, *Nucl. Data Tables* **5A**, 433 (1969).
- ⁸R. Nevald and G. Petersen, *J. Phys. F* **5**, 1778 (1975).
- ⁹T. Hioki, M. Kontani, and Y. Masuda, *J. Phys. Soc. Jpn.* **39**, 958 (1975).
- ¹⁰*Landolt-Börnstein, New Series II/8*, Supplement 1, edited by K. H. Hellwege (Springer, Berlin, 1964), p. 27.
- ¹¹P. W. Selwood, *Magnetochemistry* (Interscience, New York, 1956), p.73.
- ¹²M. Belakhovsky and D. K. Ray, *Phys. Rev. B* **12**, 3956 (1975).
- ¹³Y. Yafet and V. Jaccarino, *Phys. Rev.* **133**, A1630, (1964).
- ¹⁴*Landolt-Börnstein I/4*, edited by K. H. Hellwege (Springer, Berlin, 1955), p.529.
- ¹⁵I. A. Campbell, *J. Phys. C* **2**, 1338 (1969).
- ¹⁶A. Narath and D. W. Alderman, *Phys. Rev.* **143**, 328 (1966).
- ¹⁷J. A. Seitchik, V. Jaccarino, and J. H. Wernick, *Phys. Rev.* **138**, A148 (1965).
- ¹⁸A. Narath, in *Hyperfine Interactions*, edited by A. J. Freeman and R. B. Frankel (Academic, New York, 1967), p. 354.
- ¹⁹A. J. Freeman and R. E. Watson, in *Magnetism IIA*, edited by G. T. Rado and H. Suhl (Academic, New York, 1965), p. 291.
- ²⁰K. Samwer, thesis, University of Göttingen, 1981 (unpublished).
- ²¹S. R. Nagel and J. Tauc, *Phys. Rev. Lett.* **35**, 380 (1975).
- ²²J. Tauc and S. R. Nagel, *Comments Solid State Phys.* **7**, 69 (1976).
- ²³S. R. Nagel and J. Tauc, in *Proceedings of the 3rd Conference On Liquid Metals, Bristol—1977*, edited by B. Cantor (Chameleon, London, 1978).
- ²⁴F. R. Szofran, G. R. Gruzalski, J. W. Weymouth, D. J. Sellmyer, and B. C. Giessen, *Phys. Rev. B* **14**, 2160 (1976).
- ²⁵A. J. Kerns, D. E. Polk, R. Ray, and B. C. Giessen, *Mater. Sci. Eng.* **38**, 49 (1979).
- ²⁶K. H. J. Buschow, *J. Appl. Phys.* **52**, 3319 (1981).
- ²⁷I. Ansara, A. Pasturel, and K. H. J. Buschow, *Phys. Status Solidi A* **69**, 00 (1982).
- ²⁸U. Mizutani, K. T. Hartwig, T. Massalski, and R. W. Hopper, *Phys. Rev. Lett.* **41**, 661 (1978).
- ²⁹P. Panissod, D. Aliaga Guerra, A. Amamou, J. Durand, W. L. Johnson, W. L. Carter, and S. J. Poon, *Phys. Rev. Lett.* **44**, 1465 (1980).